Rh/γ-Al_2O_3 catalytic layer integrated with sol–gel synthesized microporous silica membrane for compact membrane reactor applications

Sreekumar Kurungot, Takeo Yamaguchi *, and Shin-ichi Nakao

Department of Chemical System Engineering, The University of Tokyo, 7-3-1 Hongo, Bunkyo-ku, Tokyo 113, Japan

Received 1 October 2002; accepted 17 December 2002

An efficient and compact catalytic membrane reactor for reforming of CH_4 was developed by integrating a hydrogen perm-selective silica membrane with an Rh/γ-Al_2O_3 catalyst layer. The catalytic layer was sandwiched between the outer surface of the α-Al_2O_3 support tube and the silica membrane with an aim of improving the heat and mass transfer rates through the system and to simplify the reactor geometry. The system showed improved efficiency for reforming of CH_4 at comparatively lower operating temperatures and steam to C molar ratios than the conventional fixed-bed steam reforming systems. Under optimized conditions, a nearly 25–30% improvement from the equilibrium conversion level was achieved as a result of abstraction of hydrogen from the product stream by the silica membrane integrated with the catalyst layer. The performance of the system was evaluated as a function of various process parameters. Because of the compactness and efficiency, the present system emerges as a promising alternative to the conventional membrane reactors, which possess separate catalytic and membrane units.

KEY WORDS: inorganic membrane; membrane reactor; steam reforming; silica membrane.

1. Introduction

Recently, there has been great interest in developing catalytic membrane reactors (CMR) for producing hydrogen from the naturally abundant hydrogen feedstocks such as CH_4, because of the growing concern over infrastructure and energy density [1]. Even though steam reforming (STR), catalytic partial oxidation (CPO) and autothermal reforming (ATR) are established processes for commercial applications, the requirement for high operating temperatures, particularly for STR, and the existence of a large temperature gradient along the catalyst bed make industrial applications of these processes cumbersome [2–4]. The process efficiencies and target are determined largely by thermodynamics of the reactions as a result of the limitations imposed by the thermodynamic equilibrium of the associated reactions. On the other hand, by performing the reactions in well-designed CMRs, they permit simultaneous reaction and separation and, therefore, enhancement of conversion in thermodynamically limited reactions can be achieved [5,6].

Even though Pd and some of its alloys display 100% hydrogen perm-selectivity, the permeability values of such membranes are low compared with the high catalytic reaction rates [7,8]. Microporous silica has been recognized as an alternative to Pd systems owing to its high perm-selectivity and permeation values for hydrogen and also its low cost [9,10]. However, the conventional membrane reactor approach of integrating a packed catalyst bed with a hydrogen perm-selective membrane has limitations for reasons such as a low mass transfer rate through the membrane compared with the high reaction rate in the catalyst bed and the existence of a temperature gradient in the catalyst zone [4]. Recognizing these facts, we have attempted to execute a different approach by integrating the reforming catalyst as a layer along with the hydrogen perm-selective silica membrane, which is expected to improve process efficiency, make the CMR system more compact and reduce the overall cost. The selection of the catalyst is very important. The commercially available Ni-based STR catalysts are vulnerable to coking and sintering [11]. Moreover, the high Ni loadings (>10% metal) of such systems cannot guarantee the required mechanical stability of the catalyst layer. Tsuru *et al.*, in a recent study, tried to perform membrane reforming of CH_4 by dispersing NiO inside the pores of the α-Al_2O_3 hanger tubes, but could not prevent deactivation even after performing the reaction at steam/C ratios of 5–10 [10]. On the other hand, noble metal catalysts are reported to be more coke resistant (except Pt) in addition to their comparatively high thermal stability due to low metal loading (usually <2% metal) [12,13]. Among these, supported Rh catalysts are reported to be very active in the conversion of CH_4 *via* STR or POX. In the case of Rh supported on Al_2O_3, the active site for

* To whom correspondence should be addressed.
E-mail: yamag@chemsys.t.u-tokyo.ac.jp

1011-372X/03/0300-0273/0

CH_4 adsorption is reported to the partially oxidized Rh surface; moreover, the CH_4 adsorption rate is decreased significantly owing to removal of oxygen from the catalyst [14,15]. However, addition of small amounts of air along with steam during reforming can replenish the oxygen loss due to the high adsorption rate of oxygen on Rh [16]. In this paper, we discuss the synthesis of a silica membrane integrated Rh/γ-Al_2O_3 catalyst system, where the catalyst layer is sandwiched between the membrane and α-Al_2O_3 support tube, and its application in designing a compact membrane reactor to facilitate reforming of CH_4 under moderate operating conditions such as atmospheric pressure, low steam to C molar ratio and moderate reaction temperatures.

2. Experimental

2.1. Preparation of catalytic membrane

Boehmite (γ-AlOOH) sol was prepared by using the standard recipe reported elsewhere [17]. A solution of $RhCl_3 \cdot 2H_2O$ (1 wt%) and poly(vinyl alcohol) (PVA) (1 wt%) were added to the sol, and the boehmite concentration was adjusted either by evaporation or by dilution with deionized water (the concentration of the final sol was 1 wt% Rh in 0.6 mol l^{-1} of boehmite in PVA). The sol was used for dip-coating the outer surface of an α-Al_2O_3 tube (pore size $\sim$0.1 μm; length 3.5 cm; top part sealed), which was fixed on a dense ceramic tube by glass sealing. The dip-coated layer was dried at 50 °C and calcined at 600 °C at a heating and cooling rate of 25 °C h^{-1}. We repeated the dip-coating and calcination steps twice to obtain a crack-free layer of Rh/γ-Al_2O_3. Polymeric silica sol was prepared by hydrolysis and condensation of tetraethyl orthosilicate (TEOS) in ethanol with HNO_3 as catalyst [18]. Dilute HNO_3 (1 mol l^{-1} solution) was added slowly to a mixture of known quantities of ethanol (Wako Pure Chemical Industries) and TEOS (Aldrich Chemical) with gentle stirring. The mixture was kept at room temperature for about 30 min. Subsequently, the temperature of the mixture was raised slowly to 70 °C and at this temperature the mixture was refluxed for 3 h to obtain the sol of the desired quality. The silica sol was diluted to a concentration of 0.1 mol l^{-1} using ethanol. The α-Al_2O_3 tube, with the Rh/γ-Al_2O_3 surface was immediately dipped into the silica sol (dipping time 10 s) and dried at 40 °C in a humidity-controlled oven with 60% RH. Finally, the sample was calcined at 600 °C in a temperature-controlled furnace to obtain a thin layer of silica over the catalyst layer.

2.2. Membrane reactor

The catalytic membrane obtained was loaded in a reactor for permeation studies and reforming experiments. The set-up of the membrane reactor, as shown in figure 1, consists of a furnace with provision for mounting the catalytic membrane. The feed can be delivered through the tubular part of the catalytic membrane tube using mass-flow controllers. Permeation occurs through the α-Al_2O_3–Rh/γ-Al_2O_3–silica interfaces, or in other words the active silica layer was situated at the permeate side of the membrane. Permeate side vacuum conditions were used to measure the permeation of the gases through the membrane. The gas permeation was calculated from the rate of increase of pressure in the downstream side measured with a Baratron pressure sensor. Permeation values were standardized with units of mol m^{-2} s^{-1} Pa^{-1}. While performing reforming experiments, the permeate side was connected to the sweep gas inlet. Both the permeate and retentate fluxes were separately analyzed by using an on-line gas chromatograph fitted with active carbon

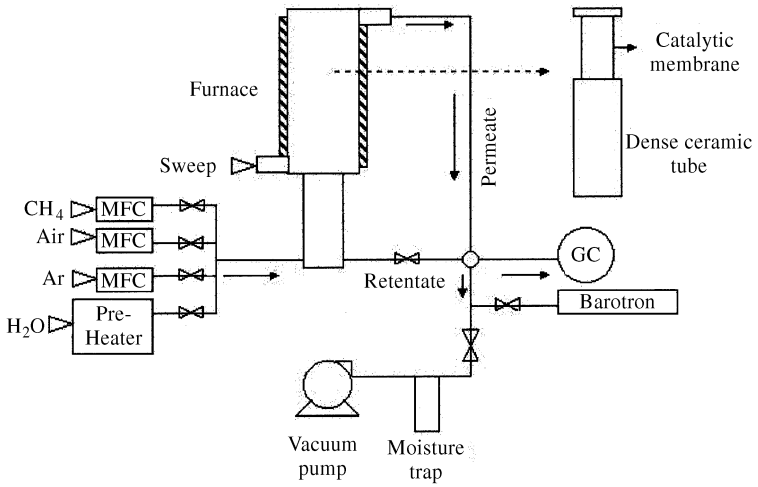

Figure 1. Process flow diagram of the catalytic membrane reactor set-up used for performing permeation studies and reforming experiments.

column and thermal conductivity detector to measure the total CH_4 conversion.

3. Results and discussion

3.1. Physical characteristics

Membrane characteristics such as thickness and continuity were observed with a Hitachi S-900 FESEM by scanning a cross-section of the catalytic membrane. The silica and the intermediate $Rh/\gamma\text{-}Al_2O_3$ layers possess thicknesses of 1.5 and 9 μm, respectively, as is evident from the FESEM image shown (figure 2). The BET surface area, pore diameter and XRD data for $Rh/\gamma\text{-}Al_2O_3$ and the parent $\gamma\text{-}Al_2O_3$ materials were obtained by analyzing the respective powdered samples prepared by calcining the original boehmite and Rh incorporated boehmite sols. The BET surface area and pore diameter data were obtained by N_2 sorption method using a Micromeritics surface area analyzer. The $\gamma\text{-}Al_2O_3$ and $Rh/\gamma\text{-}Al_2O_3$ materials displayed surface areas of 272 and 284 $m^2\,g^{-1}$, respectively. The $\gamma\text{-}Al_2O_3$ and $Rh/\gamma\text{-}Al_2O_3$ displayed average pore diameters of 4.1 and 4.3 nm, respectively, indicating that Rh particles are dispersed in the $\gamma\text{-}Al_2O_3$ matrix without obviously changing the microstructure of the latter. Therefore, as in the case of pure $\gamma\text{-}Al_2O_3$, Rh incorporated $\gamma\text{-}Al_2O_3$ can also serve as an efficient supporting layer for forming a silica membrane by dip coating the surface of the layer with standard silica sol prepared by the sol–gel route. Figure 3 represents the XRD pattern of $Rh/\gamma\text{-}Al_2O_3$ material (Philips PW 1710 X-ray diffractometer; CuKα radiation). The characteristic XRD peaks observed for Rh_2O_3 (114) and (110) planes at 2θ values 33 and 36° were broad and small, indicating highly dispersed Rh_2O_3 particles in the $\gamma\text{-}Al_2O_3$ matrix. The calculated particle size of Rh_2O_3, using Scherrer's equation, was 4.4 nm.

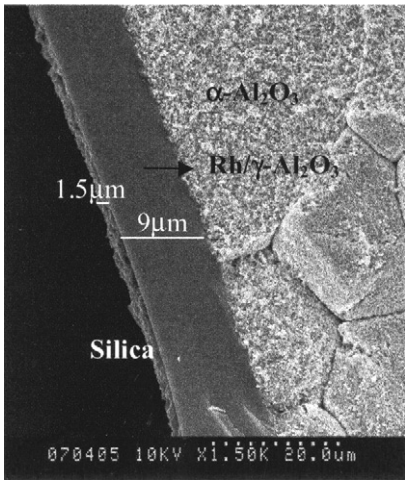

Figure 2. FESEM image of the cross-section of the $\alpha\text{-}Al_2O_3$ tube coated with $Rh/\gamma\text{-}Al_2O_3$ and silica layers.

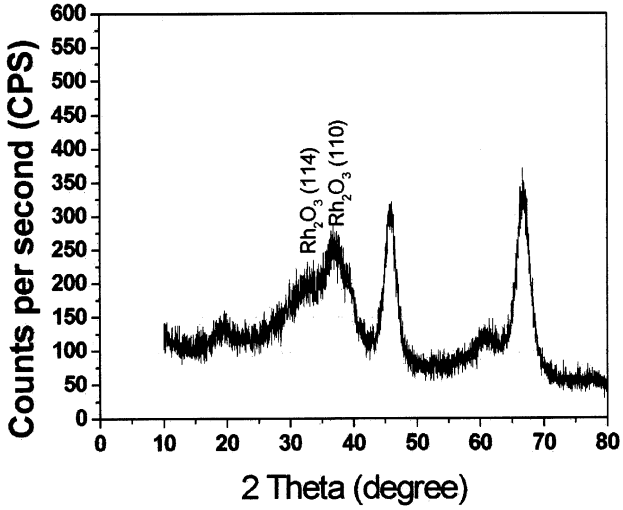

Figure 3. X-ray diffraction pattern of $Rh/\gamma\text{-}Al_2O_3$.

3.2. Permeation properties

Single-component permeances of the H_2 and CH_4 along with the H_2/CH_4 separation factor as a function of temperature are presented in table 1. H_2, with a kinetic diameter of 2.8 Å, showed activated transport, with its permeance increased from 9.28×10^{-8} mol $m^{-2}\,s^{-1}\,Pa^{-1}$ at 100 °C to 3.01×10^{-7} mol $m^{-2}\,s^{-1}\,Pa^{-1}$ at 525 °C. However, in the case of CH_4 permeation (kinetic diameter = 3.7 Å), temperature variations did not lead to significant change in its permeance. The large difference in the permeation values of H_2 and CH_4 clarifies the microporous nature of the silica layer, the majority of its pores having dimensions <3.7 Å. As a net effect of the difference in the permeation properties of H_2 and CH_4, the separation factor for H_2 to CH_4 increased with increase in temperature. The separation factor for H_2 to CH_4, which was nearly 7.5 at 100 °C, increased progressively with increase in temperature and was ~31 at 525 °C. The hydrogen permeation was activated with an apparent activation energy of 6.8 kJ mol^{-1}. The activation energy for permeance is considered as a useful extra parameter to explain the membrane quality; higher hydrogen activation energy reflects the small pore

Table 1
Gas transport data for H_2 and CH_4 over the silica-based $Rh/\gamma\text{-}Al_2O_3$ catalytic membrane

Temperature (°C)	Permeation (mol $m^{-2}\,s^{-1}\,Pa^{-1}$)		Separation factor H_2/CH_4
	H_2	CH_4	
100	9.28×10^{-8}	1.24×10^{-8}	7.5
200	1.54×10^{-7}	1.14×10^{-8}	14
300	1.94×10^{-7}	1.10×10^{-8}	18
400	2.35×10^{-7}	1.09×10^{-8}	22
500	2.85×10^{-7}	1.05×10^{-8}	27
525	3.01×10^{-7}	0.96×10^{-8}	31

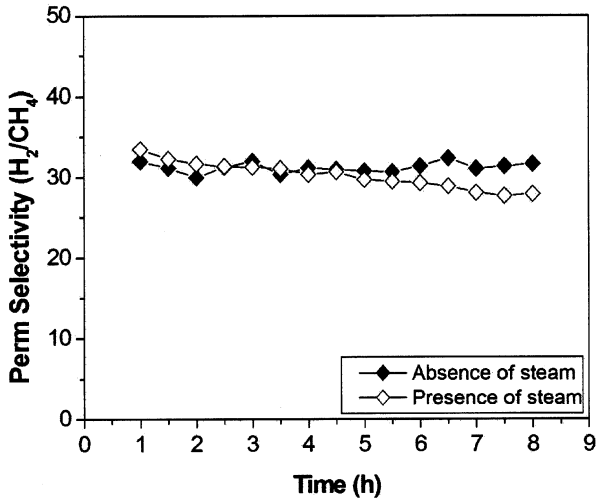

Figure 4. Variation of H_2/CH_4 perm-selectivity as a function of time in the presence and absence of steam. Operating temperature 550 °C; $H_2:CH_4:H_2O$ ratio 1:1:3.5.

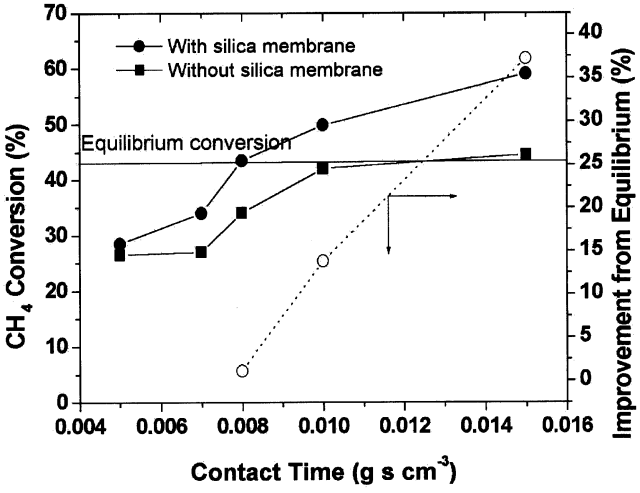

Figure 5. Effect of contact time on methane conversion and improvement over the equilibrium level for silica-based catalytic membrane with the intermediate catalytic layer of $Rh/\gamma\text{-}Al_2O_3$. Reaction temperature 525 °C; H_2O/C molar ratio 3.5.

sizes involved. The value of the activation energy is roughly in agreement with those reported for high-performance silica membranes [19,20].

In order to understand the hydrothermal stability of the silica membrane, a stability test was carried out at 550 °C by keeping the feed molar ratios of $H_2:CH_4:H_2O$ at 1:1:3.5. The experiment was performed for 8 h, and the H_2/CH_4 perm-selectivity was measured at intervals of 30 min. An identical experiment under dry conditions was also performed. The results, as presented in figure 4, indicate a very slow drop in the perm-selectivity value (H_2/CH_4) during the experiment in a humid atmosphere. Generally, at high temperatures (usually above 600 °C), silica interacts with steam and causes densification of the material. A perfect hydrothermally stable silica membrane would be an ideal choice for membrane reactor purposes; however, in the temperature range of our choice (*i.e.*, $\leq$550 °C), the membrane did not show a rapid change in permeation characteristics and, thereby, severely influence the performance of the membrane reactor set-up.

3.3. *Reforming of methane*

CH_4, diluted with Ar and air to a volume of 30% and O/C (where "C" represents carbon in CH_4) molar ratio of 1.0, was supplied along with steam to perform the reforming reaction at atmospheric pressure. An N_2 sweep in the rate of 30 $cm^2\,min^{-1}$ was maintained in the permeate side to facilitate H_2 transfer. The reaction was performed in the temperature range 400–575 °C by maintaining different H_2O/C molar ratios and contact times. Generally, a mass balance in the range 92–94% was measured during the experiments.

CH_4 conversion was monitored over the catalytic membrane and also over the $Rh/\gamma\text{-}Al_2O_3$ layer without the silica membrane layer over it at 525 °C using an H_2O/C molar ratio of 3.5 at various contact times (*i.e.*, the time of contact of the reactant mixture per gram of $Rh/\gamma\text{-}Al_2O_3$ catalyst). The results are presented in figure 5. The effect of H_2 removal on conversion is demonstrated more explicitly in the same figure by plots of improvement over the equilibrium level for the catalytic membrane. The results clearly display an improved performance of the system at high contact times, where the conversions obtained were considerably higher than the equilibrium level. CH_4 conversion, which was very close to the equilibrium conversion level of 43% at a contact time of 0.008 g s cm^{-3}, registered a value of 50% at a contact time of 0.01 g s cm^{-3} with a net improvement of more than 16% from the equilibrium value. The conversion reached nearly 59.5% at a contact time of 0.015 g s cm^{-3}, giving a net improvement from the equilibrium level by 37%. However, with further increase in contact time, we observed color change of the catalytic membrane from light yellow to gray, probably due to carbon deposition into the micropores as a result of increased rate of CH_4 decomposition as a side reaction at very high contact time. When the contact time was $\leq$0.007 g s cm^{-3}, there was no improvement from the equilibrium level. Hence the results lead to the conclusion that the system can be operated very efficiently in the contact time region 0.008–0.015 g s cm^{-3}. It should be noted that in the absence of the silica layer (*i.e.*, with only the $Rh/\gamma\text{-}Al_2O_3$ layer), the conversion was either lower than or very close to the equilibrium value in the contact time region 0.005–0.015 g s cm^{-3}. This implies that the small selectivity for H_2 over CH_4, known as Knudsen selectivity, caused by the microstructure of the $Rh/\gamma\text{-}Al_2O_3$ layer is not sufficient to drive the reaction above the thermodynamic equilibrium level. Hence the results presented in figure 5

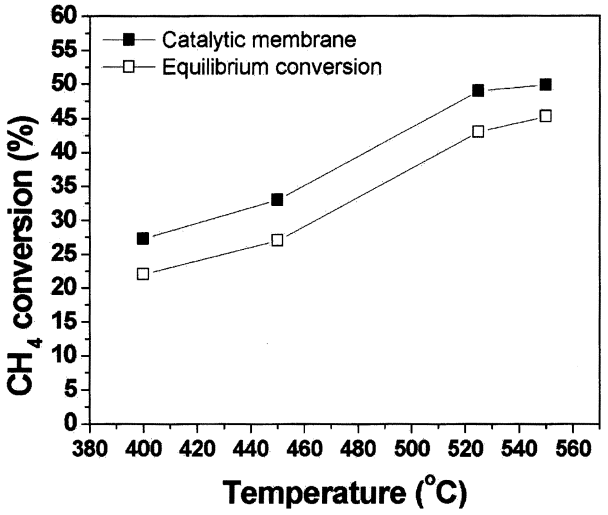

Figure 6. Influence of reaction temperature on methane conversion during reforming of methane. H_2O/C molar ratio 3.5; contact time 0.01 g s cm^{-1}.

demonstrate very well the superior performance of the integrated system.

The temperature effect in CH_4 conversion was monitored by performing the reaction in the temperature range 400–550 °C at an H_2O/C molar ratio of 3.5. Even though conversion was maximum at a contact time of 0.015 g s cm^{-3}, for the temperature effect studies we selected an intermediate contact time value of 0.01 g s cm^{-3} with the aim of minimizing any possible deactivation effect, which otherwise would counteract the results since the experiment requires prolonged exposure time to cover the selected temperature regions in the range 400–550 °C. As can be seen from figure 6, satisfactory improvement was obtained in the temperature range 400–525 °C and thereafter the margin of the improvement decreased progressively with increasing reforming temperature. It must be noted that since both the α-Al_2O_3 support and the Rh/γ-Al_2O_3 intermediate layer were Knudsen diffusing, their resistivity is expected to increase as the temperature increases. The progressive drop in the rate of movement of the feed mixture through the Knudsen diffusing layer, as a result of increase in resistivity, is expected to increase concomitantly the residence time of the reactants with the catalyst layer. However, the extent of improvement slightly decreased after 525 °C, contrary to expectations. A possible reason for this detrimental effect could be the drastic drop in water vapor permeation through the substrate due to low absorption rate. Any preferential fall in water permeation to a degree larger than the drop in CH_4 permeation, which will obey Knudsen law, may lead to a reduction in H : C ratio with increase in temperature and therefore a drop in efficiency, as detailed in the following section.

The data presented in table 2, which shows the influence of H_2O to C molar ratios on CH_4 conversion in an experiment in the temperature range 500–550 °C

Table 2
Influence of H_2O/C molar ratio on CH_4 conversion (contact time 0.015 g s cm^{-3})

Temperature (°C)	CH_4 conversion (%)	
	$H_2O/C = 2.5$	$H_2O/C = 3.5$
500	31.6	46.4
525	34.2	58.7
550	39.3	59.5

using a contact time of 0.015 g s cm^{-3}, display the additional advantage of enhanced conversion while operating the reaction at high steam to C molar ratios. Generally, an H_2O to C molar ratio of a minimum of 2.5 is desirable to avoid coke deposition. The CH_4 conversion, which was ~34% at 525 °C and an H_2O/C molar ratio of 2.5, increased to ~59.5% as the H_2O/C molar ratio increased to 3.5, with substantial improvement from the equilibrium level. Considering the resistance imparted by the interfaces, the stoichiometrically required H_2O/C molar ratio in the vicinity of the catalyst side is available by maintaining a slightly higher ratio than that stoichometrically required in the feed side. CH_4 reacts very effectively with steam under such conditions and part of CO produced during the reaction subsequently reacts with steam by the water gas shift (WGS) reaction, leading to a high CH_4 conversion and better H_2 yield. *In situ* removal of H_2 by the membrane enhances the rate of both of these reactions. Enhancement in the rate of CO removal by the WGS reaction can reduce coke deposition caused by the so-called Boudouard reaction. Based on the results obtained from this study, the minimum required H_2O/C molar ratio for process efficiency can be taken as 3.5.

4. Conclusion

By integrating a hydrogen perm-selective silica layer with a reforming catalytic layer of Rh/γ-Al_2O_3, an efficient and compact catalytic membrane reactor for reforming of CH_4 was developed. The system showed improved efficiency for reforming of CH_4 at comparatively lower operating temperatures and steam to C molar ratios than in the conventional fixed-bed steam reforming systems. The process efficiency to a large extent depends on various process parameters. Under optimized reaction conditions, substantial improvement over the equilibrium conversion level was achieved as a result of abstraction of hydrogen from the product stream by the silica membrane integrated with the catalyst layer. Hence the system offers a promising alternative to the conventional membrane reactors containing separate membrane and packed-bed catalyst units.

Acknowledgments

We gratefully acknowledge NEDO for financial support and Dr. B.N. Nair of Noritake Company for fruitful discussions.

References

[1] E. Kikuchi, Catal. Today 56 (2000) 97.
[2] K.H. Hofstand, J.H.B.J. Hoebink, A. Holmen and G.B. Marin, Catal. Today 40 (1998) 157.
[3] D.J. Moon, K. Sreekumar, S.D. Lee, B.G. Lee and H.S. Kim, Appl. Catal. A 215 (2001) 1.
[4] J.N. Armor, J. Membr. Sci. 147 (1998) 217.
[5] E. Kikuchi, Y. Nemoto, M. Kajiwara, S. Uemiya and T. Kojima, Catal. Today 56 (2000) 75.
[6] K. Jarosch and H.I. de Lasa, Chem. Eng. Sci. 54 (1999) 1455.
[7] J.S. Oklany, K. Hou and R. Hughes, Appl. Catal. A 170 (1998) 13.
[8] K.A. Peterson, C.S. Nielsen and S.L. Laegsgaard, Catal. Today 46 (1998) 193.
[9] R.M. de Vos and H. Verweij, Science 279 (1998) 1710.
[10] T. Tsuru, T. Tsuge, S. Kubota, K. Yoshida, T. Yoshioka and M. Asaeda, Sep. Sci. Tech. 36 (2001) 3721.
[11] M.C.J. Bradford and M.A. Vannice, Catal. Rev. Sci. Eng. 41(1) (1999) 1.
[12] J.R. Rostrup-Nielsen and J.-H.-B. Hasnen, J. Catal. 144 (1993) 38.
[13] K. Seshan, H.W. Ten Barge, W. Halley, A.N.J. van Keulsen and J.R.H. Ross, in: *Natural Gas Conversion II*, eds. H.E. Curry-Hide and R.F. Howe (Elsevier, Amsterdam, 1994), pp. 285–290.
[14] D. Wang, O. Dewaele and G.F. Froment, J. Mol. Catal. A 136 (1998) 301.
[15] D.A. Hickman and L.D. Schmidt, AIChE J. 39 (1993) 1164.
[16] D.F. Padowitz and S.J. Sibener, Surf. Sci. 254 (1991) 125.
[17] B.J.R. Uhhorn, K. Keizer and A.J. Burggraaf, J. Membr. Sci. 66 (1992) 259.
[18] B.N. Nair, K. Keizer, W.J. Elferink, M.J. Gilde, H. Verweij and A.J. Burggraaf, J. Membr. Sci. 116 (1996) 161.
[19] R.M. de Vos and H. Verweij, J. Membr. Sci. 143 (1998) 37.
[20] J.C. Daniz da Costa, G.Q. Lu, V. Rudolph and Y.S. Lin, J. Membr. Sci. 198 (2002) 9.